

seen in Figure 3, the logarithms of the oxygen dissociation rates are inversely proportional to  $pK_3$ , with the chelated hemes, myoglobin, and hemoglobin all showing about the same dependence of  $K^O_2$  on  $pK_3$ . The oxygen on rates are less sensitive than the off rates. In myoglobin the on rates are about half as sensitive as the off rates, while the chelated heme on rates show no regular dependence on substituent. Appropriate data are not available for the hemoglobin tetramer. Although there is a substantial conformational or steric effect seen in the binding of oxygen to various reconstituted heme proteins, it is nonetheless the case that both the models and the proteins show the same general overall dependence of oxygen binding on substituent.

These results and the decreasing oxygen dissociation rates with increasing solvent polarity<sup>31</sup> or proximal base electron donation<sup>32</sup> agree with the conclusion that the  $Fe^{\delta+}-O-O^{\delta-}$  has considerable charge separation, placing more electron density on the oxygen

atoms. Theoretical calculations indicate that, although there is only a small negative charge on the oxygen ligand, the oxy complex has a larger amount of electron transfer into the oxygen than does the carbonmonoxy complex into the carbon monoxide, in qualitative agreement with our findings.

### Conclusions

Side chain electron donation in chelated hemes decreases oxygen dissociation rate constants but has little or no effect on association rates of oxygen or carbon monoxide or dissociation rates of carbon monoxide. Although changes in the side chain heme substituents in heme proteins sometimes cause steric effects, the general trends of such substituent effects in heme proteins are similar to those in model compounds.

**Acknowledgment.** We are grateful to the National Institutes of Health for support of this research, Grants AM07233 and HL13581, for Fellowship support (D.K.W. 1F32 CA06143-01), and for support of the computer (Grant RR-00757) and NMR (Grant RR-0708) facilities. We also thank the National Science Foundation, Grant CHE 79-50003.

(31) (a) Chang, C. K.; Traylor, T. G. *Proc. Natl. Acad. Sci. U.S.A.* **1975**, *72*, 1166-1170; (b) Traylor, T. G. In "Bioorganic Chemistry", Vol. 4; Van Tamelen, E. E., Ed.; Academic Press: New York, 1978, pp 437-468.

(32) Chang, C. K.; Traylor, T. G. *J. Am. Chem. Soc.* **1973**, *95*, 8477-8479.

## Fluorescence Detected Circular Dichroism of Proteins with Single Fluorescent Tryptophans

Eric W. Lobenstine, William C. Schaefer, and Douglas H. Turner\*<sup>1</sup>

Contribution from Department of Chemistry, University of Rochester, Rochester, New York 14627. Received November 14, 1980

**Abstract:** The first fluorescence detected circular dichroism (FDCD) measurements on proteins are reported. The proteins studied were adrenocorticotrophic hormone, glucagon, human serum albumin, monellin, and ribonuclease T1. All contain a single, fluorescent tryptophan. FDCD, transmission circular dichroism, and absorption spectra are combined to calculate the FDCD equivalent of the Kuhn dissymmetry factor,  $g_F$ . Values obtained for  $g_F$  range from  $-1 \times 10^{-3}$  for human serum albumin to  $1.65 \times 10^{-3}$  for monellin compared with  $4 \times 10^{-4}$  for free tryptophan. The N-F pH-dependent transition of human serum albumin is monitored by this technique. The data demonstrate the sensitivity of FDCD to the tryptophan environment.

The first fluorescence detected circular dichroism<sup>2-5</sup> (FDCD) measurements on proteins are reported. FDCD is combined with transmission circular dichroism (CD) and absorption measurements to give an FDCD equivalent of the Kuhn dissymmetry factor,  $g_F$ .<sup>6</sup> Due to radiationless energy transfer, this is a measure of the chirality around the fluorescent tryptophan and any chromophores that transfer energy to it. The proteins studied were adrenocorticotrophic hormone, glucagon, human serum albumin, monellin, and ribonuclease T1. All contain a single, fluorescent tryptophan. These proteins have been previously studied by fluorescence quenching techniques.<sup>7-9</sup> The  $g_F$  spectra measured are consistent with expectations based on the reported fluorescence

quenching parameters. The results demonstrate that FDCD is a sensitive, selective probe of local conformation around tryptophan in proteins.

### Experimental Section

**Methods. FDCD Spectra.** The quantity measured in FDCD is  $\theta_F^\circ = -28.65 (F_L - F_R)/(F_L + F_R)$ , where  $F_L$  and  $F_R$  are the fluorescence intensities excited by left and right circularly polarized light (LCPL and RCPL), respectively. Spectra were measured on a Cary 60 spectropolarimeter with Model 6001 CD accessory, modified for fluorescence detection (see Figure 1). Light from a xenon arc lamp is dispersed through a double-prism monochromator. The slits were fixed at 2.2 mm, resulting in a spectral bandwidth ranging from 5.9 nm at 290 nm to 1.6 nm at 210 nm. The monochromatic light is rendered plane polarized by a Glan-Thompson crystal polarizer and then made alternately left and right circularly polarized by a Pockels cell operated as a variable-wavelength quarter wave retarder. The Pockels cell modulation voltage is controlled by a linear Helipot, driven by the wavelength scanning mechanism. This control voltage is also used for computer digitization as a signal proportional to wavelength. Experimentally, perfect circular polarization is never achieved. To minimize the linearly polarized component of the light, the Pockels cell is on a laser mirror mount for precise angular adjustment. The alternating LCPL and RCPL is then absorbed by the sample which is contained in a 1-cm, cylindrical CD cell. For the experiments reported here, the resulting fluorescence was collected by two Hamamatsu R375 photomultiplier tubes (PMTs) perpendicular to the excitation beam and to each other. Scattered excitation light was blocked by Wratten 18-A filters (see Figure 1). The fluorescence emission from

(1) Alfred P. Sloan Fellow.

(2) Turner, D. H.; Tinoco, I.; Maestre, M. F. *J. Am. Chem. Soc.* **1974**, *96*, 4340.

(3) Turner, D. H. In "Methods in Enzymology"; C. H. W. Hirs, C. H. W., Timasheff, S. N., Eds.; Academic Press: New York, 1978; Vol. 49G, Chapter 8.

(4) Tinoco, I.; Turner, D. H. *J. Am. Chem. Soc.* **1976**, *98*, 6453.

(5) Tinoco, I.; Ehrenberg, B.; Steinberg, I. Z. *J. Chem. Phys.* **1977**, *66*, 916.

(6)  $g_F$  is defined by analogy to Kuhn, W. *Trans. Faraday Soc.* **1930**, *26*, 293-308.

(7) Eftink, M. R.; Ghiron, C. A. *Biochemistry* **1976**, *15*, 672-680.

(8) Eftink, M. R.; Ghiron, C. A. *Proc. Natl. Acad. Sci. U.S.A.* **1975**, *72*, 3290-3294.

(9) Eftink, M. R.; Ghiron, C. A. *Biochemistry* **1977**, *16*, 5546-5551.

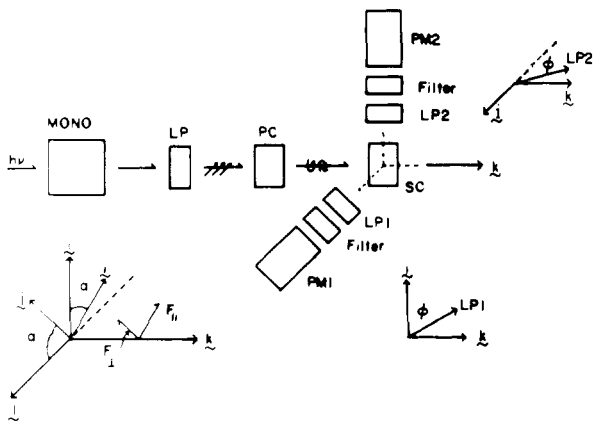


**Figure 1.** A block diagram of the FDCD instrument. MONO is the double-prism, scanning monochromator; LP, a Glan-Thompson crystal polarizer; PC, the Pockels cell; SC, a 10-mm pathlength, 22-mm o.d. cylindrical CD sample cell. LP1 and LP2 are HNP'B Polaroid polarizers, which may be removed.  $\phi$  for LP1 and LP2 are measured in the  $ik$  and  $jk$  planes, respectively. PM1 and PM2 are photomultipliers. The vectors  $i'$  and  $j'$  are in the  $ij$  plane.

the proteins studied is dominated by tryptophan emission, with direct tyrosine fluorescence contributing less than 20% of the total emission.<sup>10,11a-c,12</sup> The Wratten filters preferentially block tyrosine fluorescence by a factor of 3 over tryptophan fluorescence, and we therefore neglect it in the analysis. Due to signal-to-noise limitations, no polarizers were employed in front of the PMTs. This is equivalent to measuring spectra with linear polarizer oriented at  $45^\circ$  ( $\phi = 45^\circ$  in Figure 1). The anode current from each PMT consists of a varying current,  $I_{AC}$ , and a relatively constant current,  $I_{DC}$ .  $I_{AC}$  and  $I_{DC}$  are proportional, respectively, to the difference ( $F_L - F_R$ ) and sum ( $F_L + F_R$ ) of fluorescence intensities excited by LCPL and RCPL.  $I_{DC}$  is kept constant by feedback to the individual PMT high-voltage supplies. After amplification and conversion to voltages, the AC and DC signals are summed separately. The AC component is synchronously amplified, and signals proportional to  $I_{AC}$ ,  $I_{DC}$ , and wavelength are read by a PDP 11/34 computer. The value of  $I_{AC}/I_{DC}$  is then calculated and converted to  $\theta_F^y$  by using the appropriate calibration factor. The reported spectra are averages of five separate scans and were smoothed with a three-point binomial weighting function.

Previous FDCD measurements on samples with polarized fluorescence have been plagued by large artifacts due to residual linear polarization in the excitation light.<sup>13</sup> Similar artifacts are observed in Raman optical activity but have been elegantly eliminated by Hug.<sup>14</sup> The detection scheme described above is a modification of Hug's system, and its effectiveness has recently been demonstrated.<sup>15</sup> The origin of the artifact and its elimination can be understood by referring to Figure 1. Suppose the residual linear polarization is at an angle  $\alpha$  to the  $i$  axis. The light is absorbed by the sample and reemitted. We reference the emitted light to a new coordinate system formed by  $i'$ , the direction of the original linear polarization;  $k$ , the propagation vector of the excitation beam; and  $j'$ , a new vector perpendicular to both of these. Let  $F_{\parallel}$  and  $F_{\perp}$  be the amplitudes of the projections of the emitted light on the  $i'$  and  $j'$  (or  $k$ ) axes, respectively. Because the intensity of the emitted light passed by the analyzing linear polarizer at any angle,  $\phi$ , may be expressed as a weighted sum of the intensities for  $\phi = 0^\circ$  and  $\phi = 90^\circ$ , we will examine the intensity at each PMT for these two polarizer directions. A detector on  $j$  sees:

$$F_{\phi=0^\circ}^j = F_{\parallel} \cos^2 \alpha + F_{\perp} \sin^2 \alpha \quad (1a)$$

$$F_{\phi=90^\circ}^j = F_{\perp} \quad (1b)$$

(10) Weber, G. *Nature (London)* **1961**, *190*, 27; Weber, G. *Biochem. J.* **1961**, *79*, 29.

(11) Estimated from spectra presented in (a) Eisinger, J. *Biochemistry* **1969**, *8*, 3902; (b) Edelhoch, H.; Lippoldt, R. E. *J. Biol. Chem.* **1969**, *244*, 3876; (c) Morris, J. A.; Martenson, R.; Deibler, G.; Cagan, R. H. *J. Biol. Chem.* **1973**, *248*, 534.

(12) Longworth, J. W. *Photochem. Photobiol.* **1968**, *7*, 587; Yamamoto, Y.; Tanaka, J. *Biochim. Biophys. Acta* **1970**, *207*, 522.

(13) Lobenstine, E. W.; Turner, D. H. *J. Am. Chem. Soc.* **1979**, *101*, 2205-2207.

(14) Hug, W.; Surbeck, H. *Chem. Phys. Lett.* **1979**, *60*, 186; Hug, W. *Appl. Spectrosc.* **1981**, *35*, 115-124.

(15) Lobenstine, E. W.; Turner, D. H. *J. Am. Chem. Soc.* **1980**, *102*, 7786-7787.

Similarly, a detector on  $i$  sees:

$$F_{\phi=0^\circ}^i = F_{\parallel} \sin^2 \alpha + F_{\perp} \cos^2 \alpha \quad (2a)$$

$$F_{\phi=90^\circ}^i = F_{\perp} \quad (2b)$$

If the angle,  $\alpha$ , changes from the left to the right circularly polarized cycles, ( $F_L - F_R$ ) from each PMT will contain a term due to this linear polarization unless  $\phi = 90^\circ$ . This term is not dependent on the optical activity of the sample and is therefore an artifact. However, summing the output of the two PMTs gives:

$$\sum F_{\phi=0^\circ} = F_{\parallel}(\cos^2 \alpha + \sin^2 \alpha) + F_{\perp}(\sin^2 \alpha + \cos^2 \alpha) = F_{\parallel} + F_{\perp} \quad (3a)$$

$$\sum F_{\phi=90^\circ} = 2F_{\perp} \quad (3b)$$

The fluorescence intensity due to residual linear polarization sums to a constant, regardless of  $\alpha$ , for each half-cycle of the modulation. The difference ( $F_L - F_R$ ) now subtracts away this constant, and no artifact appears. The sum ( $F_L + F_R$ ) still contains an artifact term, but it can be made small with proper alignment of the Pockels cell.

FDCD base lines were obtained by turning off the Pockels cell modulation voltage and scanning the excitation wavelengths as usual. This zero modulation base line corrects for scatter in the sample and stray light in the cell compartment.

The FDCD spectrometer is calibrated with 10-*d*-camphorsulfonic acid (CSA). A 1-cm cell containing 1 mg/mL of CSA is placed in the excitation beam before the sample cell, which is filled with optically inactive sodium fluorescein. The fluorescein concentration is about  $6 \times 10^{-4}$  M, and all photons *not* absorbed by the CSA standard are absorbed by the fluorescein. The fluorescein fluorescence provides a *direct* measure of the CSA transmission CD. The spectrometer is then adjusted to give an ellipticity of 304 mdeg at 291 nm.

**Other Spectra.** Absorbance data were obtained on a Cary 118C spectrophotometer. Data at individual wavelengths were read from the digital readout. Spectral bandwidth of the light was less than 1 nm. Fluorescence measurements were made on a Perkin Elmer MPF-44A fluorimeter, operated in ratio mode, using excitation and emission bandwidths of 10 nm. The fluorescence depolarization ratio was defined and measured according to the method described by Parker.<sup>16</sup> A Polacoat and an HNP'B polarizer, both from Polaroid Corp., were used in the excitation and emission paths, respectively. CD measurements were made on a JASCO J-40 spectropolarimeter interfaced with a PDP 11/34 computer. The spectral bandwidth was 2 nm, and calibration was with CSA. All monochromators (including Cary 60) were wavelength calibrated using a Corning CS3-138 holmium oxide filter.<sup>17</sup> This was particularly important for absorption measurements, since absorbance appears as an exponent in the equation relating FDCD, CD, and absorption to  $g_F$  (see eq 4b).

**Materials.** Human serum albumin (HSA), ribonuclease T1 (*Aspergillus oryzae*), and L-tryptophan were obtained from Sigma Chemical Co., monellin (*Dioscoreophyllum cumminsii*) from Worthington Biochemical Corp., and glucagon from Calbiochem. Adrenocorticotrophic hormone (ACTH, porcine, an Armour product) was obtained as Acthar (corticotropin for injection). All were used without further purification. Sodium dodecyl (lauryl) sulfate (NaDodSO<sub>4</sub>), Sequal grade, was from Pierce Chemical Corp. This NaDodSO<sub>4</sub> had much lower levels of fluorescent impurities than other grades, which exhibited fluorescence emission from 310 to 400 nm. Water was deionized and doubly distilled; all other materials were reagent grade. Phosphate buffers were used because of their low absorbance in the far ultraviolet.

## Results

FDCD spectra are shown in Figure 2 for HSA and Figure 3 for ACTH, glucagon, monellin, and ribonuclease T1. Interpretation of these spectra in terms of molecular parameters depends upon the polarization of the observed fluorescence.<sup>4,5</sup> Therefore, fluorescence depolarization measurements were made on each protein. Below 250 nm, the polarization of fluorescence was always less than 0.06, indicating essentially isotropic fluorescence. Above 250 nm, only ribonuclease T1 and monellin have significant  $g_F$  bands. In the wavelength regions of these bands, the polarization of fluorescence was 0.1 or less. Thus the long-wavelength bands are significantly, but not completely, depolarized. However, it

(16) Parker, C. A. "Photoluminescence of Solutions"; Elsevier: New York, 1968; p 301.

(17) Gordon, A. J.; Ford, R. A. "The Chemist's Companion"; Wiley-Interscience: New York, 1972; p 214.

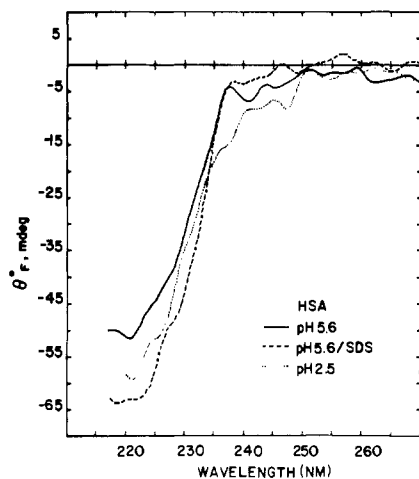


**Figure 2.** FDCD spectra of  $2.5 \times 10^{-6}$  M HSA in 0.02 M phosphate buffer: (—) pH 5.6, (···) pH 2.5, (---) HSA/NaDodSO<sub>4</sub> complex, pH 5.6. NaDodSO<sub>4</sub> concentration is  $5 \times 10^{-5}$  M. Values of  $\theta_F^\circ$  were essentially zero from 260 to 290 nm. Error limits are roughly  $\pm 3$  mdeg.

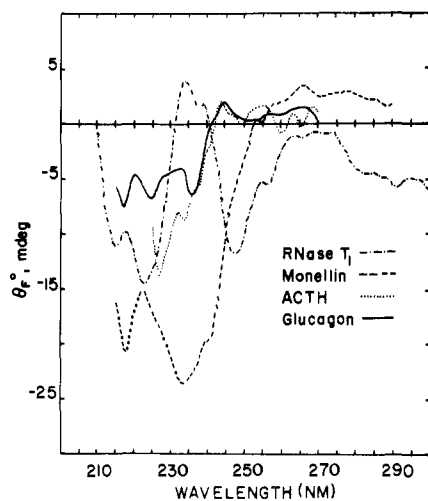


**Figure 3.** FDCD spectra of proteins in 0.01 M Tris: (—)  $2.5 \times 10^{-4}$  M glucagon, 0.1 M NaCl, pH 5.3; (---)  $9 \times 10^{-6}$  M monellin, pH 6.9; (···)  $7 \times 10^{-6}$  M ribonuclease T1, pH 6.9; (---)  $2 \times 10^{-6}$  M ACTH, pH 6.9. Values of  $\theta_F^\circ$  for glucagon and ACTH were essentially zero from 260 to 290 nm. Error limits are roughly  $\pm 3$  mdeg.

has been shown theoretically<sup>5</sup> and experimentally<sup>13,15</sup> that the FDCD signal will be identical with that observed for isotropic fluorescence, if the fluorescence detected has a polarization angle  $\phi = 35.25^\circ$  (see Figure 1). Since all the spectra reported here were measured without a polarizer, they correspond to  $\phi = 45^\circ$ . The proximity of  $35^\circ$  and  $45^\circ$ , coupled with the substantial depolarization of the long-wavelength bands, suggests it is a reasonable approximation to analyze the spectra as if they were obtained under isotropic conditions. The possibility of polarization artifacts is still present, however. Thus the 2-PMT detection system is necessary.

The theory of FDCD for isotropic fluorescence has been presented previously.<sup>2-4</sup> An important result is that

$$g_F = 2 \left( \frac{28.65R - \theta_F^\circ}{28.65 - R\theta_F^\circ} \right) \quad (4a)$$

$$R = \frac{A_L(1 - 10^{-A_R}) - A_R(1 - 10^{-A_L})}{A_L(1 - 10^{-A_R}) + A_R(1 - 10^{-A_L})} \quad (4b)$$

where  $\theta_F^\circ$  is the FDCD signal, in degrees;  $A_L$  and  $A_R$  are the sample absorbances for LCPL and RCPL, respectively, and can be obtained by measuring the CD and absorbance spectra of the sample. We call  $g_F$  the FDCD dissymmetry factor. If all the fluorescence is due to absorption by one chromophore, then  $g_F = \Delta\epsilon_F/\epsilon_F$ , the

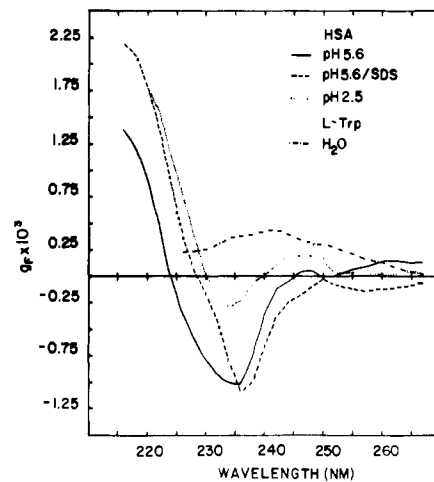


**Figure 4.** Spectra of  $g_F$  for  $5 \times 10^{-5}$  M L-tryptophan in water (---) and for tryptophan in HSA (see Figure 2): (—) pH 5.6, (···) pH 2.5, (---) HSA/NaDodSO<sub>4</sub>, pH 5.6. HSA spectra calculated from FDCD, CD, and absorption data, using eq 4. L-Tryptophan spectrum calculated from CD and absorption data alone.

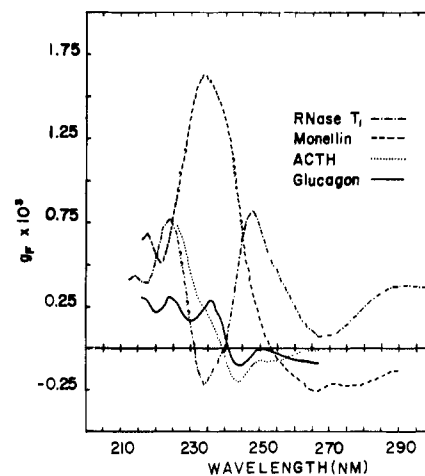


**Figure 5.** Spectra of  $g_F$  for the tryptophan in glucagon (—), monellin (---), RNase T1 (---), and ACTH (···), calculated from FDCD, CD, and absorption data, using eq 4. See Figure 3 for details.

Kuhn dissymmetry factor for that chromophore. For the proteins studied here, essentially all the detected fluorescence originates from the single tryptophan residue, but energy transfer to that residue can be important. In this case:

$$g_F = (C_F \Delta\epsilon_F + \sum_j a_j \Delta\epsilon_j C_j) / (C_F \epsilon_F + \sum_j a_j \epsilon_j C_j) \quad (5)$$

where  $C_F$ ,  $\Delta\epsilon_F$ , and  $\epsilon_F$  are the concentration, molar CD, and molar extinction coefficient of tryptophan;  $C_j$ ,  $\Delta\epsilon_j$ , and  $\epsilon_j$  are similar quantities for chromophores transferring energy to tryptophan;  $a_j$  is the average probability of transfer of energy from chromophore  $j$  to the tryptophan. In this case,  $g_F$  is a measure of the chirality around the fluorescent tryptophan and any chromophores that transfer energy to it. The contribution from energy transfer partly depends on the fraction of fluorescence that originated from absorption by a donor. For the proteins studied here, it is reasonable to assume the donor is predominantly tyrosine. An estimate for the fraction of fluorescence due to energy transfer can be obtained from approximating the fraction of absorption due to tyrosine and tryptophan, and the average probability of transfer. The values of Longworth<sup>18</sup> give the following estimates for the energy transfer contribution for absorption at 280 nm: ACTH (14%), glucagon (13%), RNase T1 (46%), and HSA (57%). Data are not available for monellin.

(18) Longworth, J. W. In "Excited States of Proteins and Nucleic Acids"; Steiner, R. F., Weinryb, I., Eds.; Plenum Press: New York, 1971; Chapter 6, pp 432-435.

Table I. Acrylamide Quenching Parameters Measured by Eftink and Ghiron<sup>7,9</sup>

protein	$k_{SV}$ , M <sup>-1</sup>	$V$ , M <sup>-1</sup>	$10^{-9}k_q$ , M <sup>-1</sup> s <sup>-1</sup>	$E_a$ , kcal/ mol	$\Delta S^\ddagger$ , eu
RNase T1	1.0	~0	0.25	9.0	10.0
HSA, pH 5.5	3.3	0.8	0.55	2.7	-9.5
HSA, pH 2.5	3.3	0.6	1.0	5.0	-0.5
HSA/NaDodSO <sub>4</sub>	1.0	0.6	0.2		
monellin	5.2	0.3	2.0	5.7	2.8
glucagon	10.5	1.0	3.7	4.8	1.0
ACTH	13.5	1.0	4.2		
<i>N</i> -AcTrpNH <sup>a</sup>	17.5	2.0	6.5	3.7	-1.4

<sup>a</sup> *N*-acetyl-L-tryptophanamide.

Figures 4 and 5 show  $g_F$  spectra calculated using FDCD, CD, and absorption spectra in conjunction with eq 4. The CD and absorption data are available as supplementary material (see Supplementary Material Available paragraph). For comparison, Figure 4 also shows the  $g_F$  spectrum of L-tryptophan in water as calculated from CD and absorption data alone. It has been shown previously that this is in good agreement with experimental FDCD results for L-tryptophan in water.<sup>15</sup>

### Discussion

One goal of this work was to survey the sensitivity of FDCD to the local environment near a tryptophan in a protein. The variety of spectra shown in Figures 2–5 testify to this sensitivity. These spectra also strikingly illustrate the advantages of combining FDCD, CD, and absorption spectra to calculate  $g_F$  spectra. For example, at its peak the FDCD ellipticity measured for HSA is almost a factor of 10 larger than that of the other proteins. However, the  $g_F$  values calculated for HSA are not extraordinary.

As seen in eq 5,  $g_F$  is a measure of the chirality of tryptophan plus anything that transfers energy to the tryptophan. For the proteins studied, energy transfer will be predominantly from tyrosine. Assuming random orientations, a tyrosine will transfer half its excitation to tryptophan when they are roughly 10 Å apart.<sup>19</sup> This is, therefore, a first approximation for the localization of conformational changes detected by FDCD when energy transfer is present. The region probed by FDCD is presumably even smaller when most of the fluorescence originates with tryptophan absorption, as in ACTH and glucagon.

An interesting feature of the  $g_F$  spectra is that bands are observed in regions where both tryptophan and tyrosine have low absorbance. This can be attributed to the fact that  $g_F$  is essentially  $\Delta\epsilon_F/\epsilon_F$ . Thus, a band will be predominant in  $g_F$  spectra if it has a significant chirality. It does not require a large absolute  $\Delta\epsilon$ . This means that  $g_F$  spectra are more sensitive to weak transitions than are conventional CD spectra. In this regard, it is interesting to note that several of the  $g_F$  spectra have bands centered around roughly 235 and 245 nm. The value of  $g_F$  is not constant across these bands, indicating a weak transition.<sup>6</sup> On the basis of simultaneous resolution of CD and absorption spectra from several tryptophan derivatives, Auer has suggested the presence of a band with pronounced ellipticity and small absorption in the 225–232-nm region.<sup>20</sup> By analogy with isoquinoline, he speculates this may be a <sup>1</sup>C symmetry-forbidden transition. Our observation of a band at 235 nm is consistent with this suggestion, though we cannot definitively assign the band to tryptophan because of energy transfer.

The proteins studied in this work have also been examined by Eftink and Ghiron, using acrylamide quenching of fluorescence.<sup>7–9</sup> These studies provide information about the tryptophan environment that can be compared with our FDCD results. In particular, they report collisional quenching constants,  $k_{SV}$ , static quenching constants,  $V$ , rate constants for quenching,  $k_q$ , and activation parameters for  $k_q$ ,  $E_a$ , and  $\Delta S^\ddagger$ . These are listed in Table I. The values of  $V$  and  $k_q$  are particularly helpful since

they are indicators of tryptophan exposure. In both cases, larger values imply greater exposure. In the following comparisons, we focus on  $g_F$  spectra, since they are the most sensitive to chirality.

The  $g_F$  spectra of ACTH, glucagon, and L-tryptophan all show small amplitudes, indicating little chirality for the tryptophan. The fluorescence quenching studies yield large values of  $V$  and  $k_q$ , implying substantial exposure of the tryptophan to solvent.<sup>7,9</sup> Both methods, therefore, give results that are consistent with the common view that these small molecules have no well-defined structure in solution.<sup>21,22</sup>

The  $g_F$  spectra of monellin and ribonuclease T1 are the only ones in this study that have significant bands above 265 nm (see Figure 5). Monellin also has the largest  $g_F$  maximum measured at 235 nm. Large  $g_F$  bands imply very chiral structures, so the tryptophans in monellin and ribonuclease T1 must be rigidly ordered. The fluorescence quenching data indeed indicate the tryptophan in ribonuclease T1 is deeply buried.  $V$  is too small to measure,  $k_q$  is more than 10 times lower than for exposed tryptophans, and the activation energy for collisional quenching is quite large, 9.0 kcal/mol.<sup>7,9</sup> The quenching data for monellin are less dramatic. However, it is still clear that monellin's tryptophan is less exposed than those in ACTH and glucagon. Thus, the FDCD results are again quite reasonable.

The  $g_F$  spectra and fluorescence quenching for HSA have been measured at pH 5.5 with and without NaDodSO<sub>4</sub> present and at pH 2.5. No simple correlation is found between the two methods. The  $g_F$  spectra indicate little conformational change upon addition of NaDodSO<sub>4</sub> but considerable change upon lowering the pH. The fluorescence quenching indicates significant differences between all three species. These results underline the differences between the two methods. The  $g_F$  spectra are sensitive to the local environment near the tryptophan, whereas fluorescence quenching can be affected by more distant changes in the protein matrix. Thus, for example, the decrease in  $k_q$  observed with NaDodSO<sub>4</sub> binding could result from the NaDodSO<sub>4</sub> blocking a pathway for acrylamide diffusion through the protein. The  $g_F$  spectra indicate this binding is not accompanied by a conformational change near the tryptophan. Evidently, the two techniques provide complementary information.

Consideration of the spectral changes observed in the pH-dependent transition of HSA gives insight into the origin of the observed chirality. This transition has been designated the N (pH 5.5) to F (pH 2.5) transition, and has been studied in some detail in both HSA and bovine serum albumin (BSA).<sup>23</sup> The tertiary structure of the N state consists of three barrel-like domains, with each having several regions of helical secondary structure as staves.<sup>24</sup> The tryptophan is located in a helix at the edge of one of the domains. The transition to the F state is characterized by expansion of the barrel structures, accompanied by a loss of up to 40% of the helix content.<sup>23</sup> In BSA, loss of the helix is primarily in the carboxy-terminal half of the molecule, while tryptophan is in the amino-terminal half.<sup>25</sup> Since the sequences and properties of HSA and BSA are similar,<sup>23,24</sup> it is reasonable to assume this is also true for HSA. The conformational changes in HSA produce a large decrease in the 235-nm band of the  $g_F$  spectra. Since the helical secondary structure around the tryptophan is probably retained, this suggests the  $g_F$  band observed at 235 nm for the N state arises from interactions due to tertiary structure. These interactions could include energy transfer to the tryptophan or direct perturbation of the tryptophan chirality. This interpretation is consistent with fluorescence quenching data since they indicate acrylamide has greater access to the tryptophan in the F state.

(21) Edelhoch, H.; Lippoldt, R. E. *J. Biol. Chem.* **1969**, *244*, 3876–3883.

(22) Panijpan, B.; Gratzner, W. B. *Eur. J. Biochem.* **1974**, *45*, 547–553.

(23) Foster, J. F. In "Albumin Structure, Function and Uses"; Rosenoer, V. M., Oratz, M., Rothschild, M. A., Eds.; Pergamon Press: New York, 1977; pp 53–84.

(24) Brown, J. R. In "Albumin Structure, Function and Uses"; Rosenoer, V. M., Oratz, M., Rothschild, M. A., Eds.; Pergamon Press: New York, 1977; pp 27–52.

(25) Hilah, M. C.; Harmsen, B. J. M.; Braam, W. G. M.; Joordens, J. J. M.; Van Os, G. A. *J. Int. J. Pept. Protein Res.* **1974**, *6*, 95–101.

(19) Eisinger, J.; Feuer, B.; Lamola, A. A. *Biochemistry* **1969**, *8*, 3908.

(20) Auer, H. E. *J. Am. Chem. Soc.* **1973**, *95*, 3003–3011.

The  $g_F$  spectra measured are thus qualitatively consistent with expectations based on fluorescence quenching results. In the future, it may be possible to provide more detailed interpretation of the spectra. This could be done by analogy with spectra measured for tryptophans in known environments. For example, the spectra of ACTH and glucagon may prove to be typical of tryptophan in a random coil. However, this will require measuring a library of spectra. An alternative approach is to compare measured spectra with those generated theoretically from an assumed conformation. Woody has made such calculations for tyrosine and phenylalanine but points out they are more difficult for tryptophan.<sup>26</sup> Several weak transitions are apparent in the  $g_F$  spectra reported here, indicating that it will be important to consider them in any such calculations.

The results reported here demonstrate that FDCD spectra can be measured for a single fluorescent tryptophan in a protein. The 2-PMT detection geometry essentially eliminates artifacts due to imperfect circularly polarized light. This is especially important

(26) Woody, R. W. *Biopolymers* 1978, 17, 1451-1467.

above 250 nm where the fluorescence is significantly polarized. While this polarization must be considered in making the measurement, it is reasonable to neglect it in analyzing the spectra reported here. However, this will not always be the case. Spectra were limited to wavelengths above 220 nm by signal-to-noise problems. Nevertheless, the  $g_F$  spectra are clearly sensitive to conformation. Several of them show indications of an additional strong band below 220 nm, which should also be conformationally sensitive. Thus FDCD provides a selective method for monitoring structural changes near fluorescent tryptophans.

**Acknowledgment.** This work was supported by NIH Grant GM22939. E.W.L. was an NIH Predoctoral Trainee (Grant 5T32GM07230).

**Supplementary Material Available:** Figures showing ellipticity vs. wavelength for HSA; ellipticity vs. wavelength for glucagon, monellin, ribonuclease T1, and ACTH; absorbance spectrum of HSA; and absorbance spectrum of glucagon, monellin, ribonuclease T1, and ACTH (4 pages). Ordering information is given on any current masthead page.

## Communications to the Editor

### Synthesis of Bridging Vinylideneiron Dimers Using 1,1-Dichlorocyclopropanes. Cyclopropanes as Intermediates

David F. Marten,\* Eckehard V. Dehmlow,† David J. Hanlon, M. Bilayet Hossain, and Dick van der Helm

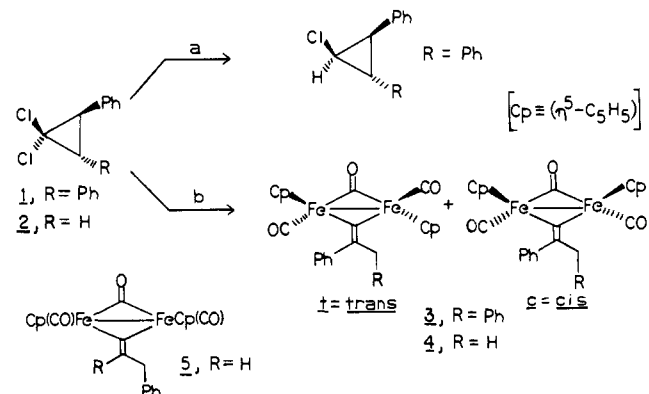
Department of Chemistry, University of Oklahoma  
Norman, Oklahoma 73019

Received February 2, 1981

Bridging alkylidene,<sup>1</sup> alkylidyne,<sup>2</sup> and vinylidene<sup>3</sup> transition-metal complexes have received intense interest recently because of their relationship to various reactions catalyzed on heterogeneous metal surfaces.<sup>4</sup> It would be extremely helpful in studying these model compounds if general and reliable routes for their syntheses were available, especially for a series of substituted derivatives. The use of alkyl substituted examples would aid in the isolation and identification of the organic and organometallic intermediates and products. We report here a general one-step synthesis of substituted bridging vinylideneiron dimers using an unusual new reaction.

In our studies related to the reducing ability of sodium  $\eta^5$ -cyclopentadienyl(dicarbonyl)ferrate (NaFp), we have found that  $Fp^-$  can be used as a selective reducing agent in the conversion of 1,1-dichlorocyclopropanes to 1-chlorocyclopropanes.<sup>5</sup> An attempt was made to simplify the procedure by eliminating the

Scheme 1<sup>a</sup>



<sup>a</sup> Reagents: (a) NaFp/THF. (b) NaOH-H<sub>2</sub>O (50:50)/THF/n-Bu<sub>4</sub>NHSO<sub>4</sub>/Fp<sub>2</sub>.

need to produce the  $Fp^-$  from  $Fp_2$  and sodium amalgam in THF. The reaction was performed instead under typical phase-transfer conditions<sup>6</sup> (NaOH-H<sub>2</sub>O (50:50), THF, n-Bu<sub>4</sub>N<sup>+</sup>HSO<sub>4</sub><sup>-</sup>) by using  $Fp_2$  directly with *trans*-1,1-dichloro-2,3-diphenylcyclopropane (1). Previous work by Alper seemed to indicate this procedure may be an alternate source of  $Fp^-$ .<sup>7</sup> The homogeneous reaction of NaFp with 1 produced a good yield of the 1-chloro-2,3-diphenylcyclopropane; however, none was observed with  $Fp_2$  under the heterogeneous conditions although all of 1 was consumed. Analysis of the product mixture showed the presence of a deep purple iron-containing substance which transformed on standing to a new red compound. The more easily purified red complex was subsequently identified as 3c by spectral<sup>8</sup> and X-ray structural

† Initial work was performed while on leave from the Technical University of Berlin, 1978. Current address: Fakultät für Chemie, Universität Bielefeld, Postfach 8640, D-4800 Bielefeld 1, Germany.

(1) For a recent review, see: Herrmann, W. A. *Angew. Chem., Int. Ed. Engl.* 1978, 17, 800. Sumner, C. E.; Riley, P. E.; Davis, R. E.; Pettit, R. J. *Am. Chem. Soc.* 1980, 102, 1752. Tebbe, F. N.; Parshall, G. W.; Reddy, G. S. *Ibid.* 1978, 100, 3611. Herrmann, W. A.; Plank, J.; Ziegler, M. L.; Balbach, B. *Ibid.* 1980, 102, 5906 and references cited therein.

(2) Herrmann, W. A.; Plank, J.; Guggolz, E.; Ziegler, M. L. *Angew. Chem., Int. Ed. Engl.* 1980, 19, 651. Nitay, M.; Priester, W.; Rosenblum, M. J. *Am. Chem. Soc.* 1978, 100, 3620.

(3) King, R. B.; Saran, M. S. *J. Am. Chem. Soc.* 1973, 95, 1811. Antonova, A. B.; Kolobova, N. E.; Petrovsky, P. V.; Lokshin, B. V.; Obezyuk, N. S. *J. Organomet. Chem.* 1977, 137, 55.

(4) Muetterties, E. L.; Stein, J. *Chem. Rev.* 1979, 79, 479. Muetterties, E. L.; Rhodin, T. N.; Band, E.; Brucker, C. F.; Pretzer, W. R. *Ibid.* 1979, 79, 91. Brady, R. C.; Pettit, R. *J. Am. Chem. Soc.* 1980, 102, 6181.

(5) Marten, D. F.; Wilburn, S. M., to be published.

(6) Dehmlow, E.; Dehmlow, S. "Phase Transfer Catalysis"; Verlag Chemie: Weinheim, 1980.

(7) Alper, H.; Paik, H.-N. *J. Am. Chem. Soc.* 1978, 100, 508.

(8) 3c: IR (heptane) 2000 s, 1968 m, 1809 s cm<sup>-1</sup>; <sup>1</sup>H NMR (CS<sub>2</sub>, 100 MHz)  $\delta$  4.26 (s, 5 H, Cp<sub>a</sub>), 4.51 (s, 2 H, CH<sub>2</sub>), 4.80 (s, 5 H, Cp<sub>b</sub>), 6.9-7.3 (m, 10 H, 2-Ph). 3t: IR (heptane) 1976 sh, 1962 s, 1809 m cm<sup>-1</sup>; <sup>1</sup>H NMR (CS<sub>2</sub>, 100 MHz)  $\delta$  4.27 (s, 5 H, Cp<sub>a</sub>), 4.57 (d, 1 H, J = 16 Hz, benzylic H), 4.72 (s, 5 H, Cp<sub>b</sub>), 4.83 (d, 1 H, J = 16 Hz, other benzylic H), 7.9-7.5 (m, 10 H, 2-Ph).